

A Versatile Method for Controlled Synthesis of Porous Hollow Spheres

Yongqiang Wang,[†] Chunjuan Tang,^{†,‡} Quan Deng,[†] Changhao Liang,[†] Dickon H. L. Ng,[§] Fung-luen Kwong,[§] Hongqiang Wang,[†] Weiping Cai,[†] Lide Zhang,[†] and Guozhong Wang^{*,†}

[†]Key Laboratory of Materials Physics, Anhui Key Laboratory of Nanomaterials and Nanotechnology, Institute of Solid State Physics, Chinese Academy of Sciences, P.O. Box 1129, Hefei 230031, P.R. China, [‡]Mathematics and Physics Department, Luoyang Institute of Science and Technology, Luoyang 471023, P.R. China, and [§]Department of Physics, The Chinese University of Hong Kong, Shatin, Hong Kong, P.R. China

Received May 8, 2010. Revised Manuscript Received July 28, 2010

A versatile method was developed to synthesize nickel silicate, silica, and silica–nickel composite porous hollow spheres by using silica spheres as templates. In the preparation, silica spheres were treated with a mixture of NiSO₄·6H₂O and NH₃·H₂O. The nickel-based ingredient reacted with the silica to form a shell while the alkaline solution could remove the silica core, thus forming the nickel silicate hollow spheres. After these spheres were further treated with hydrogen in reduction or with HCl in etching, they became silica–nickel hollow spheres or silica hollow spheres, respectively. The sizes of these hollow spheres depended on the concentration of the precursor. Our investigation also found that their surface properties or magnetic properties could be tailored by adjusting the fabrication parameters.

Introduction

The design and fabrication of inorganic hollow spheres have received considerable attention. The core–shell structures promise applications in catalysis, batteries, gas sensors, water treatment agents, encapsulation devices, controlled release of medicine, and the formation of photonic band gap crystals.^{1–6} Porous silica materials with high specific surface areas^{7–11} have been utilized in encapsulation, drug-delivery, and controlled-release applications.^{12–14} Many methods have been explored to synthesize porous silica hollow spheres, most of which are based on the

surfactant template technique.^{3,15–18} For example, porous silica-based magnetic composite particles have been synthesized through the surfactant-assisted approaches, and their products are being used in drug delivery and magnetic separation.^{19–22} The presence of surfactant is critically important in guiding the formation of the porous silica hollow spheres and silica-based composite particles. However, the size, shell thickness, and uniformity are difficult to control, especially due to the problem of agglomeration.

Silicate materials have been studied in diverse application fields owing to their structural flexibility and unique properties, including catalysis support, ion exchange, molecular adsorption, and the removal of heavy metal ions.^{23–30} Up to now, various nanostructures of silicates, such as nanowires, nanotubes, mesoporous molecular sieves, and other complex structures, have been synthesized by different methods.^{31–33} Nevertheless, the fabrication of porous silicate hollow spheres was little reported, and this

*To whom correspondence should be addressed. E-mail: gzhwang@issp.ac.cn.

(1) Pan, J. H.; Zhang, X. W.; Du, A. J.; Sun, D. D.; Leckie, J. O. *J. Am. Chem. Soc.* **2008**, *130*(34), 11256.

(2) Fei, J. B.; Cui, Y.; Yan, X. H.; Qi, W.; Yang, Y.; Wang, K. W.; He, Q.; Li, J. B. *Adv. Mater.* **2008**, *20*(3), 452–456.

(3) Wang, J. G.; Xiao, Q.; Zhou, H. J.; Sun, P. C.; Yuan, Z. Y.; Li, B. H.; Ding, D. T.; Shi, A. C.; Chen, T. H. *Adv. Mater.* **2006**, *18*(24), 3284–3288.

(4) Zhang, H. G.; Zhu, Q. S.; Zhang, Y.; Wang, Y.; Zhao, L.; Yu, B. *Adv. Funct. Mater.* **2007**, *17*(15), 2766–2771.

(5) Jiang, P.; Bertone, J. F.; Colvin, V. L. *Science* **2001**, *291*(5503), 453–457.

(6) Wu, C. Z.; Xie, Y.; Lei, L. Y.; Hu, S. Q.; OuYang, C. Z. *Adv. Mater.* **2006**, *18*(13), 1727.

(7) Kresge, C. T.; Leonowicz, M. E.; Roth, W. J.; Vartuli, J. C.; Beck, J. S. *Nature* **1992**, *359*(6397), 710–712.

(8) Brinker, C. J.; Lu, Y. F.; Sellinger, A.; Fan, H. Y. *Adv. Mater.* **1999**, *11*(7), 579–585.

(9) Ying, J. Y.; Mehnert, C. P.; Wong, M. S. *Angew. Chem., Int. Ed.* **1999**, *38*(1–2), 56–77.

(10) Zhou, Y.; Schattka, J. H.; Antonietti, M. *Nano Lett.* **2004**, *4*(3), 477–481.

(11) Raman, N. K.; Anderson, M. T.; Brinker, C. J. *Chem. Mater.* **1996**, *8*(8), 1682–1701.

(12) Botterhuis, N. E.; Sun, Q. Y.; Magusin, P. C.; van, S. R.; Sommerdijk, N. A. *Chem.—Eur. J.* **2006**, *12*(5), 1448–1456.

(13) Zhao, W. R.; Gu, J. L.; Zhang, L. X.; Chen, H. R.; Shi, J. L. *J. Am. Chem. Soc.* **2005**, *127*(25), 8916–8917.

(14) Zhu, Y. F.; Shi, J. L.; Shen, W. H.; Dong, X. P.; Feng, J. W.; Ruan, M. L.; Li, Y. S. *Angew. Chem., Int. Ed.* **2005**, *44*(32), 5083–5087.

(15) Fujiwara, M.; Shiokawa, K.; Sakakura, I.; Nakahara, Y. *Nano Lett.* **2006**, *6*(12), 2925–2928.

(16) Suh, W. H.; Jang, A. R.; Suh, Y. H.; Suslick, K. S. *Adv. Mater.* **2006**, *18*(14), 1832–1837.

(17) Wang, J. W.; Xia, Y. D.; Wang, W. X.; Poliakov, M.; Mokaya, R. *J. Mater. Chem.* **2006**, *16*(18), 1751–1756.

(18) Yu, M. H.; Wang, H. N.; Zhou, X. F.; Yuan, P.; Yu, C. Z. *J. Am. Chem. Soc.* **2007**, *129*(47), 14576–14577.

(19) Eggeman, A. S.; Petford-Long, A. K.; Dobson, P. J.; Wiggins, J.; Bromwich, T.; Dunin-Borkowski, R.; Kasama, T. *J. Magn. Magn. Mater.* **2006**, *301*(2), 336–342.

(20) Suh, W. H.; Suslick, K. S. *J. Am. Chem. Soc.* **2005**, *127*(34), 12007–12010.

(21) Wu, P. G.; Zhu, J. H.; Xu, Z. H. *Adv. Funct. Mater.* **2004**, *14*(4), 345–351.

(22) Zhou, W.; Gao, P.; Shao, L.; Caruntu, D.; Yu, M.; Chen, J.; O'Connor, C. J. *Nanomedicine* **2005**, *1*(3), 233–237.

(23) Ahmed, S.; Chughtai, S.; Keane, M. A. *Sep. Purif. Technol.* **1998**, *13*(1), 57–64.

(24) Bektas, N.; Agim, B. A.; Kara, S. *J. Hazard. Mater.* **2004**, *112*(1–2), 115–122.

(25) Corma, A. *Chem. Rev.* **1997**, *97*(6), 2373–2419.

(26) Curkovic, L.; CerjanStefanovic, S.; Filipan, T. *Water Res.* **1997**, *31*(6), 1379–1382.

(27) Gonzalez-Pradas, E.; Socias-Viciana, M.; Saifi, M.; Urena-Amate, M. D.; Flores-Céspedes, F.; Fernandez-Perez, M.; Villafranca-Sanchez, M. *Chemosphere* **2003**, *51*(2), 85–93.

(28) Kara, M.; Yuzer, H.; Sabah, E.; Celik, M. S. *Water Res.* **2003**, *37*(1), 224–232.

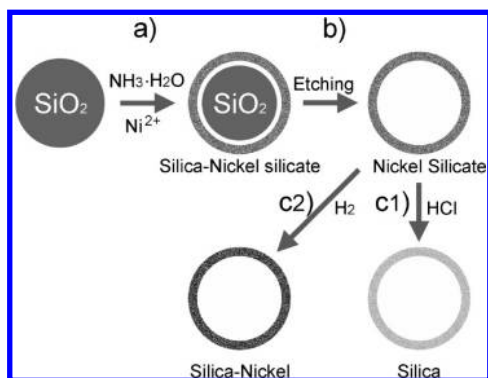
(29) Xiao, F. S.; Han, Y.; Yu, Y.; Meng, X. J.; Yang, M.; Wu, S. *J. Am. Chem. Soc.* **2002**, *124*(6), 888–889.

(30) Bouizi, Y.; Diaz, I.; Rouleau, L.; Valtchev, V. P. *Adv. Funct. Mater.* **2005**, *15*(12), 1955–1960.

(31) Hazen, R. M.; Downs, R. T.; Finger, L. W. *Science* **1996**, *272*(5269), 1769–1771.

(32) Wang, X.; Zhuang, J.; Chen, J.; Zhou, K. B.; Li, Y. D. *Angew. Chem., Int. Ed.* **2004**, *43*(15), 2017–2020.

Scheme 1. Schematic Depiction of the Synthesis Procedure of Porous Nickel Silicate, Silica, and Silica–Nickel Composite Hollow Spheres



kind of structure may have new applications.^{34–36} A new and facile synthetic method for making porous silica or silica-based composite hollow spheres with controllable surface morphology and properties is desirable.

In this work, the chemical template method is employed for the reason that the templates can directly participate in the formation of the shell wall, thus simplifying the surface modification procedures. Silica spheres were often used as a physical template to prepare hollow spheres through coating and subsequently removing themselves in alkaline conditions.^{37,38} The dissolving property of silica spheres in alkaline conditions enlightens us to use silica spheres as a chemical template. Ammonia provided hydroxide ions continually based on the ionization of ammonia, which can dissolve the surface of the silica spheres through breaking the silicon–oxygen bonds and form the silicate ions. The silicate ions further reacted with the nickel ions to form nickel silicate particles in situ around the residual silica cores. When the silica cores were removed by etching, the nickel silicate hollow spheres could be obtained. Here, the nickel ions were provided slowly from the release of nickel ammonia complex ions in ammonia solution, which could avoid the deposition of nickel ions in alkaline conditions. We also demonstrated that the obtained nickel silicate hollow spheres could be transformed into silica and silica–nickel composite hollow spheres through different controlled ways.

The synthesis procedure of the porous nickel silicate, silica, and silica–nickel composite hollow spheres is depicted in Scheme 1: (a) The silica spheres were prepared by the Stöber method,³⁹ and they were placed in an ammonia solution that contained nickel ions. Initially, a silica core–nickel silicate shell structure was obtained. (b) After the silica cores were removed by dissolving in sodium hydroxide solution, the nickel silicate hollow spheres were produced, which could be further transformed into silica hollow spheres by selective leaching of nickel ions in acid solution (c1) and silica–nickel composite hollow spheres by using in situ reduction in a hydrogen atmosphere (c2). The performance of porous nickel silicate hollow spheres in absorbing the methylene

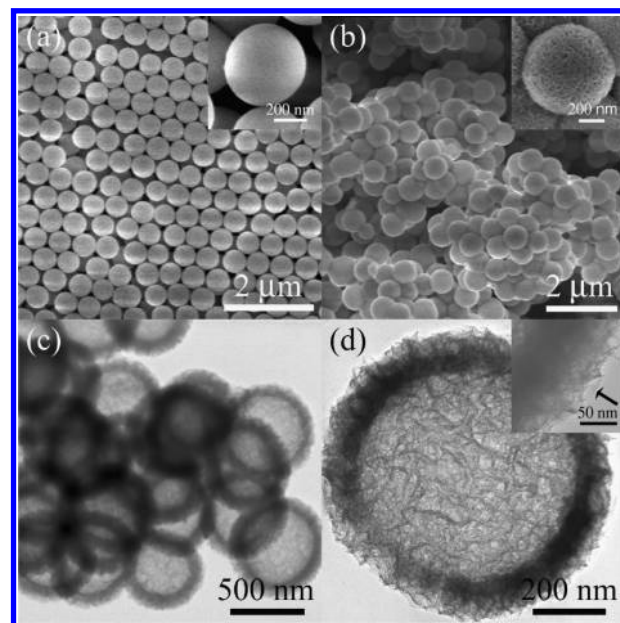


Figure 1. SEM images of (a) silica colloidal spheres and (b) nickel silicate hollow spheres; their insets are the magnified images. TEM images of (c) nickel silicate hollow spheres and (d) a magnified image of a sphere in part c; the inset is the shell of the hollow sphere.

blue (MB) dye solution was evaluated. The surface properties of the as-obtained porous silica hollow spheres and the magnetic properties of the as-obtained silica–nickel hollow spheres were also studied.

Experimental Section

A typical synthesis of the nickel silicate hollow spheres is as follows. Uniform silica spheres were prepared by the Stöber method. Analytical grade $\text{NiSO}_4 \cdot 6\text{H}_2\text{O}$ (7.5 mmol) was mixed with a 40 mL aqueous solution of ammonia ($\text{NH}_3 \cdot \text{H}_2\text{O}$, 28%, 10 mL) to form a homogeneous solution under stirring. A 1.6 g portion of silica spheres was put into 20 mL of deionized water before it was mixed with the prepared mixture. The final mixture was transferred into a Teflon autoclave (80 mL) before it was heated at 90 °C for 12 h in a water bath under stirring. After cooling to room temperature, a green precipitate (silica–nickel silicate core–shell spheres) was found. In order to remove the silica core from the product, the green precipitate is dispersed in 50 mL of sodium hydroxide solution (1 M) and stirred for 16 h. The nickel silicate hollow spheres were washed with distilled water and dried at 60 °C for 12 h.

To prepare the silica hollow spheres, 0.1 g of the nickel silicate hollow spheres was dispersed in hydrochloric acid solutions of different concentrations (4, 2, and 1 M), and the colloidal solution was stirred at 80 °C for 6 h. After cooling to room temperature, the silica hollow spheres which appeared in white color were washed with distilled water before being dried at 60 °C for 12 h.

To prepared silica–nickel composite hollow spheres, 0.1 g of the nickel silicate hollow spheres were placed in a ceramic boat in the middle of a horizontal tube furnace. Hydrogen was allowed to flow (30 mL min^{-1}) in the horizontal tube oven at 450 °C for different durations (0.5, 1.5, and 6 h). Black powder was collected in the ceramic boat at room temperature.

In characterization, the phase of the products was analyzed by X-ray diffraction (XRD), in a 2θ range from 10 to 80°, using $\text{Cu K}\alpha$ radiation (Philips X'pert diffractometer). The morphologies of the as-prepared products were studied by field emission scanning electron microscopy (FESEM, Sirion 200 FEG) and high-resolution emission transmission electron microscopy (HRTEM, JEOL-2010, 200 kV) with an energy-dispersive X-ray analyzer

(33) Wang, X.; Zhuang, J.; Peng, Q.; Li, Y. D. *J. Solid State Chem.* **2005**, *178*(7), 2332–2338.

(34) Wang, Y.; Wang, G.; Wang, H.; Liang, C.; Cai, W.; Zhang, L. *Chem.—Eur. J.* **2010**, *16*(11), 3497–3503.

(35) Zhuang, Y.; Yang, Y.; Xiang, G.; Wang, X. *J. Phys. Chem. C* **2009**, *113*(24), 10441–10445.

(36) Wang, Y.; Wang, G.; Wang, H.; Cai, W.; Zhang, L. *Chem. Commun.* **2008**, *48*, 6555–6557.

(37) Iler, R. K. *The colloid chemistry of silica and silicates*; Cornell University Press: Ithaca, NY, 1955; Chapter 2.

(38) Ren, N.; Wang, B.; Yang, Y. H.; Zhang, Y. H.; Yang, W. L.; Yue, Y. H.; Gao, Z.; Tang, Y. *Chem. Mater.* **2005**, *17*(10), 2582–2587.

(39) St, W.; Fink, A. *J. Colloid Interface Sci.* **1968**, *26*, 62–69.

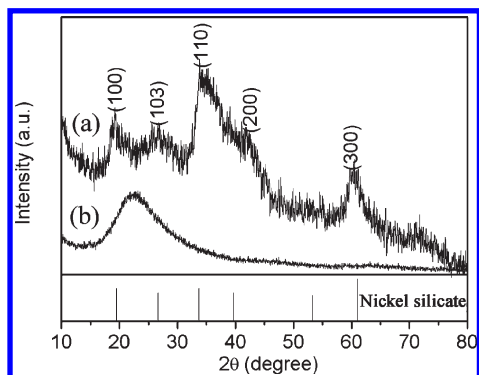


Figure 2. XRD patterns of (a) nickel silicate hollow spheres and (b) silica colloidal spheres.

(EDX, OXFORD, Link ISIS); the nitrogen adsorption/desorption curve and pore size distribution of the products were obtained by using accelerated surface area and porosimetry analyzer (Micrometrics ASAP 2020); magnetic measurements were performed with a superconducting quantum interference device (SQUID) magnetometer (Quantum Design, MPMS XL).

In the adsorption tests, MB solutions with different concentrations were used as the typical organic pollutants. The as-obtained nickel silicate hollow spheres (20 mg) were dispersed homogeneously in the MB solution (40 mL) by ultrasonication for several minutes and then kept for a specified duration (10 h) until solid and liquid separated naturally by gravitation. MB concentration was determined by UV–vis spectrophotometer (CARY-5E). The adsorption isotherm was obtained by varying the initial concentrations at room temperature.

Results and Discussion

Nickel Silicate Hollow Spheres. The SEM image of silica sphere templates is shown in Figure 1a. The diameter of silica spheres with a smooth surface is about 500 nm (see inset of Figure 1a). After hydrothermal reaction in ammonia solution containing nickel ions, a silica core coated nickel silicate shell was obtained, which can be seen clearly from the TEM and SEM images (Figure S1, Supporting Information) that each dark disk is embedding a dark circle at the center. When the silica core is dissolved in the alkaline solution, the size distribution of the product is kept uniform and the spherical shape is retained without collapse, as shown in Figure 1b. However, the surface of an individual sphere becomes coarse and porous (inset of Figure 1b). In addition, the diameter of the obtained spheres is about 700 nm, which is bigger than that of the original silica sphere templates. XRD patterns of the silica sphere templates and the nickel silicate products were shown in Figure 2. All of the peaks in Figure 2a can be identified as nickel silicate dehydrate (JCPDS 43-0664). Nickel, silicon, and oxygen elements were also detected in the EDX spectrum of the nickel silicate product in Figure S2a of the Supporting Information. These results indicated that the silica sphere templates could react with the nickel ions to form nickel silicate during hydrothermal treatment.

The nickel silicate hollow spheres are further characterized by TEM (Figure 1c and d). It is found that the sphere has a hollow structure with a shell thickness of 100 nm. The porous shell consisted of nanoscale lamella, as pointed out by the arrow in the inset of Figure 1d. Since nickel silicate has a layered clay structure, it tends to form lamella. As clearly seen from a broken hollow sphere in Figure S3 of the Supporting Information, the lamella interweave with each other during the growth process, which leads to a porous surface structure. Moreover, the size and shell thickness of nickel silicate hollow spheres can be controlled by the

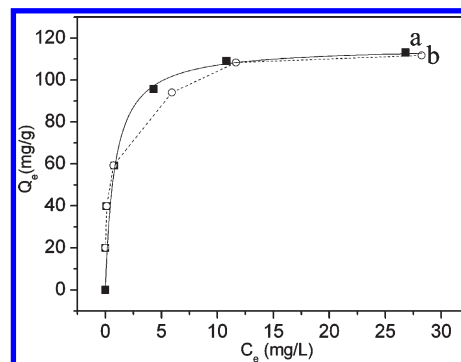


Figure 3. Adsorption isotherm of MB of (a) the new as-obtained and (b) regenerated porous nickel silicate hollow spheres.

parameters such as the diameter of the silica colloidal spheres and the amount of nickel ions. The products were demonstrated in Figures S4 and S5 of the Supporting Information.

The specific surface area of the nickel silicate hollow spheres was investigated. Figure S6 of the Supporting Information shows the nitrogen adsorption/desorption isotherms of the nickel silicate hollow spheres. The isotherm can be categorized as type IV with a distinct hysteresis loop. The BET surface area of the nickel silicate hollow spheres is determined to be $348 \text{ m}^2 \text{ g}^{-1}$.

The adsorption capability of the porous nickel silicate hollow spheres was investigated using MB, which is a common cationic dye in the textile industry. Figure 3 shows the adsorption of MB in the presence of nickel silicate hollow spheres. The correlation between the equilibrium absorption of MB (Q_e , mg g^{-1}) and the equilibrium solute concentration (C_e , mg L^{-1} , eq 1) can be described by the Langmuir adsorption model.⁴⁰

$$Q_e = Q_m b C_e / (1 + b C_e) \quad (1)$$

where Q_m (mg g^{-1}) is the maximum adsorption capacity corresponding to a complete monolayer coverage and b is the equilibrium constant (L mg^{-1}). From Figure 3a, it is evident the experimental data fits the Langmuir adsorption model quite well. The maximum adsorption capacity of the as-obtained nickel silicate is found to be 113 mg g^{-1} , which is much higher than 58 mg g^{-1} of the sepiolite in the same conditions.⁴¹ This indicates that the as-obtained porous nickel silicate hollow spheres have an excellent adsorption performance. After absorbing MB, the porous nickel silicate hollow spheres could be refreshed by combustion at $400 \text{ }^\circ\text{C}$ in air for 4 h, and the regenerated nickel silicate hollow spheres still exhibit large adsorption performance, as shown in curve b of Figure 3. The above results show that the as-obtained porous nickel silicate hollow spheres provide a novel material for the removal of pollutants in weakly biodegradable materials, which indicates the great potential for the porous nickel silicate hollow spheres to be dye removal agents.

Silica Hollow Spheres. Porous silica spheres prepared from silicate mineral spheres by the selective leaching method have been extensively studied by many researchers.^{42–44} During the leaching process, metal ions are extracted in acidic solution and a large amount of Si–OH groups are generated, while Si–OH groups are

(40) Zhong, L. S.; Hu, J. S.; Liang, H. P.; Cao, A. M.; Song, W. G.; Wan, L. J. *Adv. Mater.* **2006**, *18*(18), 2426.

(41) Dogan, M.; Ozdemir, Y.; Alkan, M. *Dyes Pigm.* **2007**, *75*(3), 701–713.

(42) Aznar, A. J.; Gutierrez, E.; Diaz, P.; Alvarez, A.; Poncelet, G. *Microporous Mater.* **1996**, *6*(2), 105–114.

(43) Temuujin, J.; Okada, K.; MacKenzie, K. J. *Appl. Clay Sci.* **2003**, *22*(4), 187–195.

(44) Wypych, F.; Adad, L. B.; Mattoso, N.; Marangon, A. A.; Schreiner, W. H. *J. Colloid Interface Sci.* **2005**, *283*(1), 107–112.

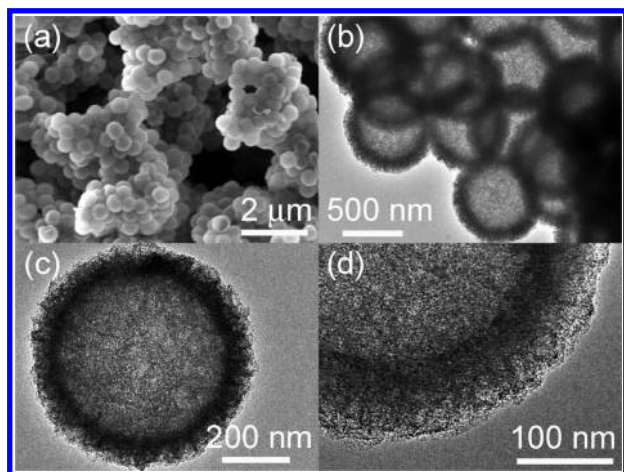


Figure 4. (a) SEM and (b) TEM images of porous silica hollow spheres, (c) a single porous silica hollow sphere, and (d) a magnified image on the bottom right of the hollow sphere.

unstable and rapidly polymerize by forming Si–O–Si bonds and leading to a silica skeleton and the final porous silica spheres. In our experiment, when the porous nickel silicate hollow spheres are treated in hydrochloric acid solution, the color of the solution would be altered from light green to white, indicating that the nickel silicate is dissolved and the silica is created. The large-scaled and uniform porous silica spheres were shown in Figure 4a, and the corresponding TEM image (Figure 4b) indicated the spherical particles exhibit a hollow structure. It can be seen clearly from the broken silica hollow spheres, as shown in Figure S7 of the Supporting Information. The magnified TEM image (Figure 4d) further proved its shell structure, which is different from the thick lamellar structure obtained from the porous nickel silicate hollow spheres. The shell thickness of porous silica spheres is about 60 nm, which is slightly thinner than that of the nickel silicate hollow spheres (Figure 1d). The shrinkage of the shell thickness is attributed to the removal of nickel ions from the nickel silicate skeleton. After the treatment in hydrochloric acid solution, the nickel peaks disappeared in the EDX spectrum of the sample (Figure S2b, Supporting Information). These results indicated that the silica hollow spheres could be successfully synthesized by the selective leaching method. In addition, the size and shell thickness of nickel silicate hollow spheres can be controlled easily, and the corresponding porous silica hollow spheres with adjustable size and shell thickness are shown in Figures S4 and S5 of the Supporting Information. Here, the leaching method provides an alternative avenue to prepare porous silica hollow spheres with controlled size and shell thickness.

The concentration effect of hydrochloric acid on the surface properties of silica hollow spheres was investigated; BET measurements have been performed to estimate the specific surface area and pore size distribution. The nitrogen adsorption/desorption isotherms of silica hollow spheres are shown in Figure S8 of the Supporting Information; all of them exhibited a type IV isotherm with a clear hysteresis loop, demonstrating these samples with the mesoporous characteristics. The specific surface areas of the silica hollow spheres were $801 \text{ cm}^2 \text{ g}^{-1}$ (4 M), $759 \text{ cm}^2 \text{ g}^{-1}$ (2 M), and $643 \text{ cm}^2 \text{ g}^{-1}$ (1 M). It was found that these specific surface areas were decreased with decreasing acid concentration; however, the pore size centered at 3.4 nm (4 M), 3.8 nm (2 M), and 5.5 nm (1 M) was increased with decreasing acid concentration (shown in Figure S4b, Supporting Information). This phenomenon may be explained as follows: When the nickel silicate was leached in acid solution, the Si–OH groups would be formed, and

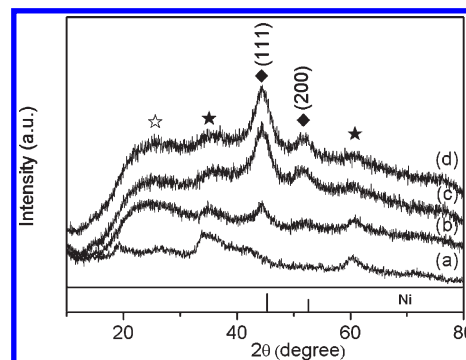


Figure 5. XRD patterns of porous silica–nickel hollow spheres obtained with different reduction times: (a) 0 h; (b) 0.5 h; (c) 1.5 h; (d) 6 h. (☆ silica; ★ nickel silicate; ◆ nickel).

the silica hollow spheres would be generated from the polymerization of Si–OH groups. Since more Si–OH groups existed in high acid concentration, the amount of silica nuclei in high acid concentration would be higher than that in low acid concentration. Thus, more silica nanoparticles would be formed in high acid concentration, and the diameter of silica nanoparticles in high acid concentration is smaller than that in low acid concentration. It is important to note that the obtained weight per each silica hollow sphere is fixed, whether in high or low acid concentration. Silica hollow spheres are aggregated by smaller silica particles, resulting in a larger surface area and smaller pore size in the same weight of spheres, and vice versa. Thus, the surface properties of porous silica spheres were greatly influenced by the acid concentration; i.e., the different BET surface area and pore size may be controlled by tuning the acid concentration.

Silica–Nickel Composite Hollow Spheres. Silica hollow spheres with magnetic properties attracted a lot of researchers for their potential usage in drug delivery. The traditional method was using magnetic nanoparticles as the precursor, but the attraction between magnetic nanoparticles makes the preparation of magnetic silica composite hollow spheres rather difficult. In this work, the nickel silicate hollow spheres were used as the precursor and were reduced in a hydrogen atmosphere, nickel ions were in situ reduced to form nickel particles, and then the silica–nickel composite hollow spheres were obtained easily.

The in situ transformation of nickel silicate hollow spheres into silica–nickel composite hollow spheres was confirmed by XRD results, as shown in Figure 5. It was found that the intensity of the broad peak around 23° and the peaks of nickel particles increased gradually with the prolonging reduction duration; meanwhile, the characteristic peaks of nickel silicate disappeared, which indicated nickel ions reduced gradually in a hydrogen atmosphere. It should be noted that the peaks of nickel silicate could still be observed after 6 h of reduction. The origin of these peaks may come from the interior core of the nickel silicate particles, since the hydrogen molecules were difficult to enter into the interior and hence some nickel silicate particles were not reduced. The morphology and size of the reductive product were shown in Figure 6a, and the smooth surface could be seen from the inset of Figure 6a. The TEM image of a single sphere still exhibits a hollow structure with a uniform shell after reduction (Figure 6b). The high magnification TEM image of a partial shell of the silica–nickel composite hollow spheres revealed that nickel particles bestrewed homogeneously in the silica matrix, which were marked by the circles in Figure 6c. The corresponding SAED pattern, as shown in Figure 6d, further suggested the formation of nickel particles. Three ring patterns with dots corresponding to

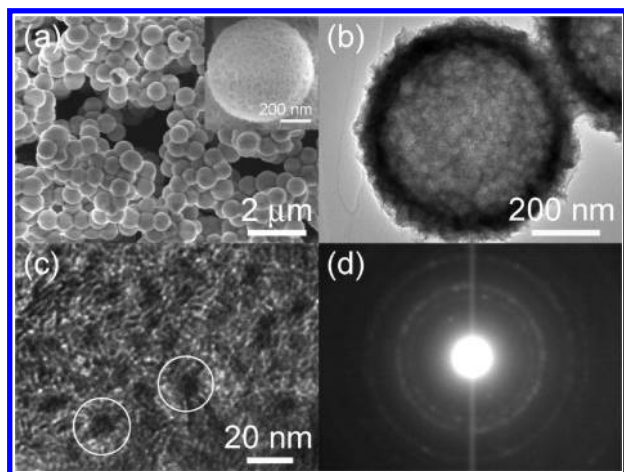


Figure 6. Images of the silica–nickel composite hollow spheres obtained after 6 h of reduction in a hydrogen atmosphere: (a) SEM image (inset shows an individual sphere); (b) TEM image; (c) high magnification TEM image of the shell; (d) the corresponding SAED pattern.

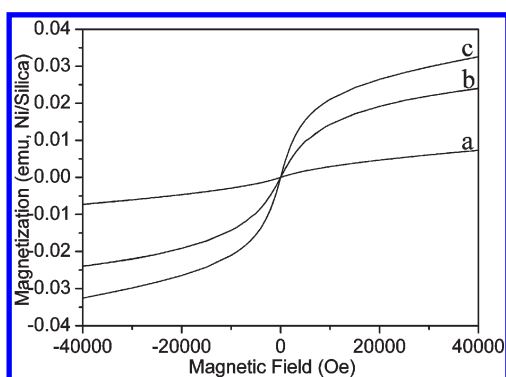


Figure 7. Room temperature field-dependent magnetization curve of silica–nickel composite hollow spheres obtained at 450 °C for different reduction times: (a) 0.5 h; (b) 1.5 h; (c) 6 h.

planar spacings of 0.203, 0.176, and 0.124 nm could be observed, which is consistent with the indices of 111, 200, and 222 of fcc nickel.^{45,46}

The effects of the reduction duration on the magnetic properties of silica–nickel composite hollow spheres are studied. The magnetization of the spheres was evaluated by using a SQUID measurement. The room temperature field-dependent magnetization curves of the samples treated in different reduction durations at 450 °C are shown in Figure 7. We find that the magnetic saturation of the silica–nickel composite hollow spheres increases with increasing reduction duration. This may be attributed to the increasing amount of nickel particles in the nickel–silica composite hollow spheres. Using zero-field cooling (ZFC) in an applied field of 100 Oe, we find evidence for the superparamagnetic behavior in these nickel–silica composite hollow spheres (6 h). The corresponding ZFC susceptibility shows a blocking temperature T_b at 16 K (Figure 8). For the nickel particles, the critical diameter to form a single-domain state is about 55 nm.⁴⁷ In this work, the average size of nickel particles embedded in the silica

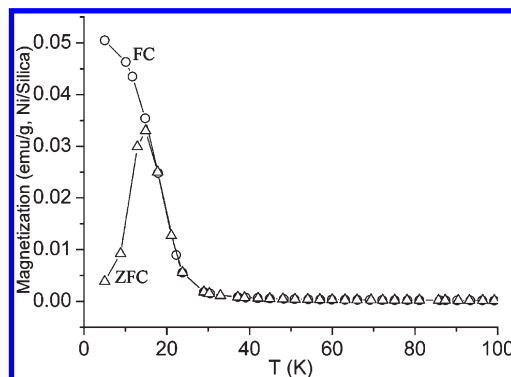


Figure 8. ZFC/FC specific magnetization in an applied field H of 100 Oe (silica–nickel hollow spheres obtained at 450 °C for 6 h).

shell is estimated to be less than 20 nm from Figure 6c. The size of nickel is below the critical diameter; thus, the silica–nickel hollow spheres are superparamagnetic. These magnetic properties possessed by the hollow spheres enable them to have possible applications in drug delivery and magnetic separations. In addition, the nickel particles generated are surrounded by the silica matrix; thus, the silica–nickel composite hollow spheres are expected to be stable in the air for a long time.²⁰

Conclusions

We have demonstrated a versatile template synthesis approach for the fabrication of porous hollow spheres with controlled properties. Porous nickel silicate hollow spheres, silica hollow spheres, and silica–nickel hollow spheres are obtained through an in situ chemical reaction. The obtained porous nickel silicate hollow spheres with large surface area could be used as a dye adsorbent and exhibit excellent removal ability. Porous silica hollow spheres obtained by leaching the porous nickel silicate hollow spheres exhibit a large surface area. The size and shell thickness of porous silica hollow spheres can be tuned by adjusting the corresponding parameters of nickel silicate hollow spheres. Nickel–silica composite hollow spheres obtained under hydrogen reduction treatment of the porous nickel silicate hollow spheres exhibit superparamagnetic properties. This template method is expected to be useful as a general tool for the synthesis of other porous hollow spheres.

Acknowledgment. This work is supported by the National Basic Research Program of China (Grant No. 2007CB936604), the Scientific Research Foundation for the Returned Overseas Chinese Scholars, State Education Ministry, the Special Foundation of President of Hefei Institutes of Physical Science, the Chinese Academy of Sciences, and the Hundred Talent Program of the Chinese Academy of Sciences.

Supporting Information Available: TEM images of a broken nickel silicate hollow sphere and a nickel silicate hollow sphere with different sizes and shell thicknesses, EDX spectra of nickel silicate and silica hollow spheres, and a nitrogen adsorption/desorption isotherm of the porous nickel silicate and silica hollow spheres. This material is available free of charge via the Internet at <http://pubs.acs.org>.

(45) Bao, J. C.; Liang, Y. Y.; Xu, Z.; Si, L. *Adv. Mater.* **2003**, *15*(21), 1832–1835.
 (46) Liu, Q.; Liu, H. J.; Han, M.; Zhu, J. M.; Liang, Y. Y.; Xu, Z.; Song, Y. *Adv. Mater.* **2005**, *17*(16), 1995.

(47) Lu, A. H.; Salabas, E. L.; Schuth, F. *Angew. Chem., Int. Ed.* **2007**, *46*(8), 1222–1244.